# Observation of Structures in the Processes $e^+e^- \to \omega\chi_{c1}$ and $\omega\chi_{c2}$

M. Ablikim *et al.*[*]
(BESIII Collaboration)

(Received 26 January 2024; revised 13 March 2024; accepted 22 March 2024; published 19 April 2024)

We present measurements of the Born cross sections for the processes $e^+e^- \to \omega\chi_{c1}$ and $\omega\chi_{c2}$ at center-of-mass energies $\sqrt{s}$ from 4.308 to 4.951 GeV. The measurements are performed with data samples corresponding to an integrated luminosity of 11.0 fb$^{-1}$ collected with the BESIII detector operating at the Beijing Electron Positron Collider storage ring. Assuming the $e^+e^- \to \omega\chi_{c2}$ signals come from a single resonance, the mass and width are determined to be $M = (4413.6 \pm 9.0 \pm 0.8)\ \mathrm{MeV}/c^2$ and $\Gamma = (110.5 \pm 15.0 \pm 2.9)$ MeV, respectively, which is consistent with the parameters of the well-established resonance $\psi(4415)$. In addition, we also use one single resonance to describe the $e^+e^- \to \omega\chi_{c1}$ line shape and determine the mass and width to be $M = (4544.2 \pm 18.7 \pm 1.7)\ \mathrm{MeV}/c^2$ and $\Gamma = (116.1 \pm 33.5 \pm 1.7)$ MeV, respectively. The structure of this line shape, observed for the first time, requires further understanding.

DOI: 10.1103/PhysRevLett.132.161901

In the past decades, charmonium physics has gained great interest from both theory and experiment, stimulated by the observations of charmoniumlike states, such as $X(3872)$, $Y(4230)$, and $Z_c(3900)$ [1–3]. These states, comprised of charm-anticharm ($c\bar{c}$) quark pairs, do not fit in the conventional charmonium spectroscopy and could be exotic states [4–7]. Above the open-charm threshold, besides the three well-known vector structures observed in the inclusive hadronic cross section, i.e., $\psi(4040)$, $\psi(4160)$, and $\psi(4415)$ [8], a few vector $Y$ states are also observed, namely, $Y(4230)$, $Y(4360)$, $Y(4500)$, and $Y(4660)$ in the hidden-charm final states [2,9–11] and $Y(4790)$ in the $D_s^{*+}D_s^{*-}$ final state [12]. The overpopulation of observed vector states compared to the expected charmonium states in this energy region implies the presence of new formation mechanisms. Some theoretical models interpret these as charmonium hybrids or tetraquark states [5–7]. More experimental measurements are needed to understand the nature of these states.

In addition, the conventional vector charmonium states above the open-charm threshold have not been understood well yet. Besides the inclusive hadronic final states, they are seldom observed in exclusive final states [8]. Especially, the $\psi(4415)$ has never been observed in any hidden-charm decay [8]. Therefore, a search for new decays is essential to enhance our understanding of these states.

The BESIII Collaboration has reported the first observation of the process $e^+e^- \to \omega\chi_{c1}$ at the center-of-mass energy $\sqrt{s} = 4.600$ GeV and $e^+e^- \to \omega\chi_{c2}$ at $\sqrt{s} = 4.420$ GeV [13]. The $\sqrt{s}$-dependent line shapes of their cross sections, however, are still absent, key information which could help us clarify the sources of these signals and gain further insights into these observed vector states. Since then, the BESIII Collaboration has collected more data in a wider center-of-mass energy range, allowing for the determination of the $e^+e^- \to \omega\chi_{c1,2}$ line shape with high precision.

In this Letter, we report studies of the processes $e^+e^- \to \omega\chi_{c1,2}$ based on the $e^+e^-$ annihilation data taken at $\sqrt{s} = 4.308$ to 4.951 GeV in 2013–2014 and 2019–2021, where $\chi_{c1,2}$ are reconstructed via the decay modes $\chi_{c1,2} \to \gamma J/\psi$, $J/\psi \to \ell^+\ell^-$ ($\ell = e, \mu$), and $\omega$ is reconstructed via its decay $\omega \to \pi^+\pi^-\pi^0$, $\pi^0 \to \gamma\gamma$.

The BESIII detector is a magnetic spectrometer [14] located at the Beijing Electron Positron Collider (BEPCII) [15]. The cylindrical core of the BESIII detector consists of a helium-based multilayer drift chamber (MDC), a plastic scintillator time-of-flight system (TOF), and a CsI (Tl) electromagnetic calorimeter (EMC), which are all enclosed in a superconducting solenoidal magnet, providing a 1.0 T magnetic field. The solenoid is supported by an octagonal flux-return yoke with resistive plate chamber muon identifier modules interleaved with steel. The acceptance of charged particles and photons is 93% over the $4\pi$ solid angle. The charged-particle momentum resolution at 1 GeV/$c$ is 0.5%, and the d$E$/d$x$ resolution is 6% for the electrons from Bhabha scattering. The EMC measures photon energies with a resolution of 2.5% (5%) at 1 GeV in the barrel (end cap) region. The time resolution of the TOF

---

[*] Full author list given at the end of the Letter.

barrel section is 68 ps, while that of the end cap section is 110 ps. The end cap TOF system was upgraded in 2015 with multigap resistive plate chamber technology, providing a time resolution of 60 ps [16]; this improvement benefits about 70% of the data sample used in this work.

This analysis is performed based on the data samples collected at 25 energy points in the range of $\sqrt{s} = 4.308$–$4.951$ GeV. The center-of-mass energy and the integrated luminosity of each sample are measured with the dimuon and Bhabha processes, respectively [17–19], as listed in Supplemental Material [20]. A GEANT4-based Monte Carlo (MC) simulation is implemented to optimize the signal selection criteria, extract the efficiencies, and study the backgrounds. The $e^+e^- \to \omega\chi_{c1,2}$ signal samples at each energy point are simulated according to the phase space model with the initial state radiation (ISR) effect taken into account.

The candidate events must comprise four good charged tracks with zero net charge and at least three photons, because the final states of the signal processes include $3\gamma\pi^+\pi^-\ell^+\ell^-$ ($\ell = e, \mu$). Here, each good charged track needs to satisfy the following criteria: The distance of closest approach to the interaction point is within 10 cm along the beam direction and 1 cm in the plane perpendicular to the beam direction. In addition, the polar angles ($\theta$) of the tracks must be within the fiducial volume of the MDC ($|\cos\theta| < 0.93$). Photon candidates are reconstructed from isolated showers in the EMC at least 10° away from the nearest charged tracks. The photon energy is required to be at least 25 MeV in the barrel region ($|\cos\theta| < 0.80$) or 50 MeV in the end cap region ($0.86 < |\cos\theta| < 0.92$). To suppress electronic noise and energy depositions unrelated to the event, the EMC cluster timing from the reconstructed event start time is further required to satisfy $0 \leq t \leq 700$ ns.

The tracks with momenta higher than 1 GeV/$c$ are identified as the leptons from $J/\psi$; otherwise, they are treated as the pions from the $\omega$ decay. Furthermore, electron candidates need to deposit an energy larger than 1 GeV in the EMC, and muon candidates less than 0.4 GeV. In order to further suppress the backgrounds and improve the mass resolutions, a five constraint (5C) kinematic fit is implemented by constraining the total four-momentum of the reconstructed particles to the total four-momentum of the colliding beams and the invariant mass of two photons to the $\pi^0$ nominal mass. If more than one combination is found among the final state particles, the one with the least $\chi^2_{5C}$ of the kinematic fit is chosen. The $\chi^2_{5C}$ is required to be less than 60.

The results at $\sqrt{s} = 4.436$ and 4.600 GeV are shown and discussed as examples in the main text due to their high signal significances. With all the event selection criteria imposed, the distributions of $M(\pi^+\pi^-\pi^0)$ versus $M(\ell^+\ell^-)$ of the candidate events are shown in Fig. 1. Clear event accumulations appear in the $\omega$ and $J/\psi$ signal regions, which are defined as [0.75, 0.81] and [3.08, 3.12] GeV/$c^2$, respectively. The $\omega$ and $J/\psi$ mass windows are about 3 times the width of signal MC shape. The efficiency of the mass windows varies from 82% to 91% depending on the collision energy. The distributions of $M(\pi^+\pi^-\pi^0)$ versus $M(\gamma J/\psi)$ after the $J/\psi$ mass window requirement are also shown in Fig. 1. Significant $\omega\chi_{c2}$ signals are observed at $\sqrt{s} = 4.436$ GeV, and the $\omega\chi_{c1}$ signals at $\sqrt{s} = 4.600$ GeV.

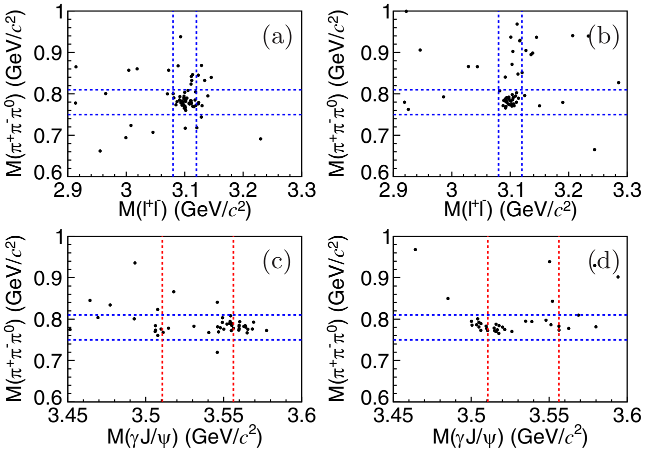

FIG. 1. Distributions of $M(\pi^+\pi^-\pi^0)$ versus $M(\ell^+\ell^-)$ for data at $\sqrt{s} = 4.436$ (a) and 4.600 GeV (b) and distributions of $M(\pi^+\pi^-\pi^0)$ versus $M(\gamma J/\psi)$ for data at $\sqrt{s} = 4.436$ (c) and 4.600 GeV (d). The blue dashed lines mark the signal regions of $\omega$ and $J/\psi$, and the red dashed lines mark the nominal masses of $\chi_{c1,2}$.

After performing the selection of the $\omega$ signal, Fig. 2 shows the corresponding one-dimensional projections on the $M(\gamma J/\psi)$ distribution which are used to extract the signal yields. The backgrounds are studied using the $\omega$-$J/\psi$ two-dimensional sideband regions defined as [0.66, 0.72] and [0.84, 0.90] GeV/$c^2$ for the $\omega$ and [3.00, 3.06] and [3.14, 3.20] GeV/$c^2$ for the $J/\psi$. No significant peaking background is observed.

For the energy points where the signal is observed with significance above $3\sigma$, an unbinned maximum-likelihood fit is performed on the $M(\gamma J/\psi)$ spectrum of selected events to determine the $\chi_{c1}$ and $\chi_{c2}$ yields. The fit function is a sum of the MC-determined $\chi_{c1}$ and $\chi_{c2}$ shapes and a flat background. Figure 2 shows the fit results at $\sqrt{s} = 4.436$

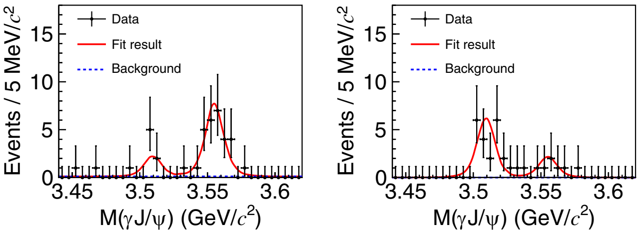

FIG. 2. Fits to the $M(\gamma J/\psi)$ distributions at $\sqrt{s} = 4.436$ (left) and 4.600 GeV (right), respectively.

and 4.600 GeV. The goodness of the fit $\chi^2/\text{n.d.f.}$ is 29.3/33 at $\sqrt{s} = 4.436$ and 27.1/33 at 4.600 GeV, where n.d.f. denotes the number of degrees of freedom. For the energy points with a signal significance less than $3\sigma$, the signal yields are obtained by directly counting the events in the $\chi_{c1}$ and $\chi_{c2}$ signal regions which are defined as [3.49, 3.53] and $[3.536, 3.576]\ \text{GeV}/c^2$, respectively. The background is estimated in the $\chi_{c1,2}$ sideband in $[3.43, 3.47]\ \text{GeV}/c^2$ and then subtracted. The results at all the energy points used in this work are summarized in Supplemental Material [20].

The Born cross section at each energy point is calculated by

$$\sigma^B(e^+e^- \to \omega\chi_{c1,2}) = \frac{N^{\text{sig}}}{\mathcal{L}_{\text{int}}\epsilon(1+\delta)\frac{1}{|1-\Pi|^2}(\mathcal{B}_e+\mathcal{B}_\mu)\mathcal{B}_1}, \tag{1}$$

where $N^{\text{sig}}$ is the signal yield, $\mathcal{L}_{\text{int}}$ is the integrated luminosity, $\epsilon$ is the selection efficiency obtained with the signal MC, $\mathcal{B}_e$ is the branching fraction $\mathcal{B}(J/\psi \to e^+e^-)$, $\mathcal{B}_\mu$ is $\mathcal{B}(J/\psi \to \mu^+\mu^-)$, $\mathcal{B}_1$ is $\mathcal{B}(\chi_{c1,2} \to \gamma J/\psi) \times \mathcal{B}(\omega \to \pi^+\pi^-\pi^0) \times \mathcal{B}(\pi^0 \to \gamma\gamma)$, $(1/|1-\Pi|^2)$ is the vacuum polarization factor [21], and $(1+\delta)$ is the radiative correction factor [22,23]. We can see the cross section is obtained using selection efficiency and radiative correction factor, which, in turn, depends on the input cross section distribution in MC simulation [24]. So the iterative procedure is used to determine the Born cross section [24]. The values of the $e^+e^- \to \omega\chi_{c1,2}$ cross sections at different energy points can be found in Supplemental Material [20].

The systematic uncertainties of the Born cross section measurements come mainly from luminosity measurement, tracking efficiency, photon detection, kinematic fit requirement, $J/\psi$ mass window, angular distribution, line shape, fit range, signal shape, background shape, and branching fraction.

The uncertainty from the luminosity measurement is about 1.0% [17–19]. The uncertainty in tracking efficiency is obtained as 1.0% per track [25], so a 4.0% uncertainty contributes to the final results. The uncertainty in photon reconstruction is about 1.0% per photon, which is estimated with a control sample of $J/\psi \to \rho^0\pi^0$ decays [26].

The uncertainty caused by the 5C kinematic fit is estimated with the method of correcting the track helix parameters, where the correction factors for $\pi$, $e$, and $\mu$ are obtained by using control samples of $e^+e^- \to \pi^+\pi^- J/\psi$, $J/\psi \to e^+e^-$, and $\mu^+\mu^-$ [27]. The difference in detection efficiency with and without the correction is taken as the systematic uncertainty. The corresponding uncertainty from the $J/\psi$ mass window cut is estimated using the control sample $e^+e^- \to \gamma_{\text{ISR}}\psi(3686)$, $\psi(3686) \to \pi^+\pi^- J/\psi$, and 1.6% is assigned as the associated systematic uncertainty [28].

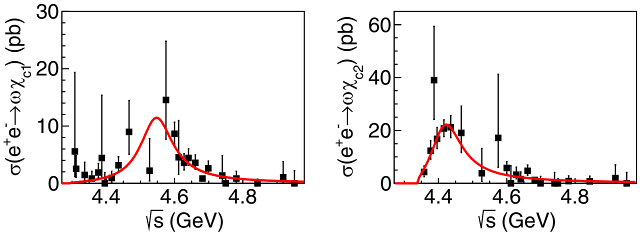

FIG. 3. Fits to the cross sections of $e^+e^- \to \omega\chi_{c1}$ (left) and $e^+e^- \to \omega\chi_{c2}$ (right) with one single resonance.

In order to estimate the uncertainty caused by the $\omega$ angular distribution in the signal simulation, the $\omega$ helicity angle function is set to $1 \pm \cos^2\theta$ in the generator instead of the phase space model, where $\theta$ is the polar angle of $\omega$ in the $e^+e^-$ rest frame. The efficiency difference between them divided by $\sqrt{12}$ is used as the systematic uncertainty [29]. For the processes $e^+e^- \to \omega\chi_{c1,2}$, single Breit-Wigner (BW) functions describe the line shapes well. To estimate the uncertainty from the line shapes, we change the mass and width of the BW functions by $\pm 1\sigma$, and the maximum change of the results is regarded as the systematic uncertainty.

To examine the systematic uncertainty due to the fits to extract the $\chi_{c1,2}$ yields, we change the fit range by $\pm 10\ \text{MeV}/c^2$, and the maximum difference between the new and nominal results is regarded as the systematic uncertainty. In order to estimate the uncertainty from the signal shape, we use the MC-determined line shape convolved with a Gaussian function as an alternative description, and the change to the fitted yield is regarded as the systematic uncertainty. In order to estimate the systematic uncertainty caused by the smooth background shape, which is constant in the nominal fit, we describe the background by a linear function, and the difference to the fitted signal yield is regarded as the systematic uncertainty. The uncertainty from the branching fractions quoted from the PDG [8] is considered as a systematic uncertainty.

All the systematic uncertainties on the $e^+e^- \to \omega\chi_{c1,2}$ cross sections are summarized in Supplemental Material [20]. The overall systematic uncertainties are obtained by adding each systematic uncertainty in quadrature under the assumption that they are independent. This results in a total systematic uncertainty of about 6%–10% for each energy point.

Figure 3 shows the $e^+e^- \to \omega\chi_{c1,2}$ dressed cross sections (the cross section without the correction for vacuum polarization, $\sigma = (\sigma^B/|1-\Pi|^2)$) at each energy point. Assuming that the $\omega\chi_{c1}$ and $\omega\chi_{c2}$ signals each come from one single resonance, we fit these cross sections with a maximum-likelihood method. In the fit, the structure is described by a BW function:

$$\sigma(\sqrt{s}) = \frac{12\pi\Gamma_{ee}\mathcal{B}(\omega\chi_{cJ})\Gamma}{(s-M^2)^2+M^2\Gamma^2} \times \frac{\Phi(\sqrt{s})}{\Phi(M)}, \tag{2}$$

where $M$ is the mass, $\Gamma$ is the total width, $\Gamma_{ee}$ is the electronic partial width, and $\Phi(\sqrt{s})$ is the two-body phase space factor. The fit results are $M_1 = (4544.2 \pm 18.7 \pm 1.7)$ MeV/$c^2$, $\Gamma_1 = (116.1 \pm 33.5 \pm 1.7)$ MeV, and $\Gamma_{ee}\mathcal{B}(\omega\chi_{c1}) = (1.86 \pm 0.32 \pm 0.13)$ eV for the $e^+e^- \to \omega\chi_{c1}$ process and $M_2 = (4413.6 \pm 9.0 \pm 0.8)$ MeV/$c^2$, $\Gamma_2 = (110.5 \pm 15.0 \pm 2.9)$ MeV, and $\Gamma_{ee}\mathcal{B}(\omega\chi_{c2}) = (3.17 \pm 0.39 \pm 0.24)$ eV for the $e^+e^- \to \omega\chi_{c2}$ process, where the first uncertainties are statistical and the second systematic as discussed later. The fit qualities are $\chi^2/\text{n.d.f.} = 25.0/22$ for $\omega\chi_{c1}$ and $\chi^2/\text{n.d.f.} = 11.9/19$ for $\omega\chi_{c2}$; both are acceptable, implying that the $e^+e^- \to \omega\chi_{c1,2}$ cross sections can be well described by a single BW function, respectively. With the current amount of data, it is unclear whether there are more resonances in these two line shapes, which needs more data to confirm. We also try to fit the $e^+e^- \to \omega\chi_{c1,2}$ cross sections using a coherent sum of BW function and phase space term and find that the phase space term does not contribute significantly. The statistical significances of the two resonances over the phase space term are $5.9\sigma$ for $e^+e^- \to \omega\chi_{c1}$ and $10.7\sigma$ for $e^+e^- \to \omega\chi_{c2}$. Taking into account systematic uncertainties decreases the significance of the structure in $e^+e^- \to \omega\chi_{c1}$ by less than $0.1\sigma$. This indicates that the structure in $e^+e^- \to \omega\chi_{c1}$ is observed for the first time. The parameters of the structure observed in $e^+e^- \to \omega\chi_{c2}$ are consistent with the known $\psi(4415)$ parameters [8].

The sources of systematic uncertainties on the resonant parameters are dominated by those due to the beam energy, BW parametrization, and cross section measurement.

We conservatively take 0.8 MeV as the systematic uncertainty in the beam energy [30] for the mass measurements of the resonances. To estimate the uncertainty from the BW parametrization, $\Gamma$ is set to be the energy-dependent width $\Gamma(\sqrt{s}) = \Gamma^0(\sqrt{s}/M)$, where $\Gamma^0$ is the nominal width of the resonance. The difference between the updated and nominal results is taken as the corresponding systematic uncertainty.

The systematic uncertainty of the cross section measurement consists of two parts: One is the uncorrelated uncertainty due to the 5C kinematic fit, line shape, and angular distribution, while the other is the common uncertainty that includes all other systematic sources mentioned above. The former part is considered by including the uncorrelated systematic uncertainty in the fit to the cross section; the change of the fitted parameter is taken as the systematic uncertainty. The latter part is common for all data points, and we simultaneously vary the cross sections at each energy point by $\pm 1\sigma$ of the systematic uncertainty. The difference between the new and nominal results is taken as the systematic uncertainty. The total systematic uncertainty is obtained by adding these two items in quadrature under the assumption that they are independent.

TABLE I. Systematic uncertainties on the resonant parameters. The first values in brackets are for the structure in $e^+e^- \to \omega\chi_{c1}$, and the second for the structure in $e^+e^- \to \omega\chi_{c2}$.

| | $\Gamma_{ee}\mathcal{B}(\omega\chi_{cJ})$ (eV) | $M$ (MeV/$c^2$) | $\Gamma$ (MeV) |
|---|---|---|---|
| Beam energy | (−, −) | (0.8, 0.8) | (−, −) |
| Parametrization | (0.01, 0.07) | (1.1, 0.2) | (0.2, 2.9) |
| Cross section | (0.13, 0.23) | (0.9, 0.1) | (1.7, 0.3) |
| Total | (0.13, 0.24) | (1.7, 0.8) | (1.7, 2.9) |

Table I summarizes all the systematic uncertainties of the resonant parameters. The overall systematic uncertainties are obtained by adding all the sources of systematic uncertainties in quadrature.

In summary, the $e^+e^- \to \omega\chi_{c1,2}$ Born cross sections have been measured at the center-of-mass energies from 4.308 to 4.951 GeV at the BESIII experiment. For each process, a nontrivial feature is observed in the cross section line shape. Under the assumption that one single resonance describes the corresponding shape, the mass and width for $e^+e^- \to \omega\chi_{c1}$ are determined to be $M = (4544.2 \pm 18.7 \pm 1.7)$ MeV/$c^2$ and $\Gamma = (116.1 \pm 33.5 \pm 1.7)$ MeV, respectively. This structure is observed for the first time with a significance of $5.8\sigma$. The mass is significantly higher compared to the structures recently observed around 4.480 GeV/$c^2$ in $e^+e^- \to K^+K^-J/\psi$ and $e^+e^- \to D^{*0}D^{*-}\pi^+$ [10,31]. It is yet unclear whether or not these two states are the same based on the currently available information, and further measurements with higher precision in this energy region will be necessary. For the $e^+e^- \to \omega\chi_{c2}$ process, the extracted parameters are $M = (4413.6 \pm 9.0 \pm 0.8)$ MeV/$c^2$ and $\Gamma = (110.5 \pm 15.0 \pm 2.9)$ MeV, suggesting that this is likely the well-known $\psi(4415)$ and implying the existence of the hidden-charm decay $\psi(4415) \to \omega\chi_{c2}$.

The BESIII Collaboration thanks the staff of BEPCII and the IHEP computing center for their strong support. This work is supported in part by National Key R&D Program of China under Contracts No. 2020YFA0406300 and No. 2020YFA0406400; National Natural Science Foundation of China (NSFC) under Contracts No. 12375071, No. 11635010, No. 11735014, No. 11835012, No. 11935015, No. 11935016, No. 11935018, No. 11961141012, No. 12022510, No. 12025502, No. 12035009, No. 12035013, No. 12061131003, No. 12192260, No. 12192261, No. 12192262, No. 12192263, No. 12192264, No. 12192265, No. 12221005, No. 12225509, and No. 12235017; Natural Science Foundation of Henan under Contract No. 242300421163; the Chinese Academy of Sciences (CAS) Large-Scale Scientific Facility Program; the CAS Center for Excellence in Particle Physics (CCEPP); Joint Large-Scale Scientific Facility Funds of the NSFC and CAS under Contract No. U1832207; CAS

Key Research Program of Frontier Sciences under Contracts No. QYZDJ-SSW-SLH003 and No. QYZDJ-SSW-SLH040; 100 Talents Program of CAS; The Institute of Nuclear and Particle Physics (INPAC) and Shanghai Key Laboratory for Particle Physics and Cosmology; European Union's Horizon 2020 research and innovation program under Marie Sklodowska-Curie grant agreement under Contract No. 894790; German Research Foundation DFG under Contract No. 455635585, Collaborative Research Center CRC 1044, FOR5327, GRK 2149; Istituto Nazionale di Fisica Nucleare, Italy; Ministry of Development of Turkey under Contract No. DPT2006K-120470; National Research Foundation of Korea under Contract No. NRF-2022R1A2C1092335; National Science and Technology fund of Mongolia; National Science Research and Innovation Fund (NSRF) via the Program Management Unit for Human Resources & Institutional Development, Research and Innovation of Thailand under Contract No. B16F640076; Polish National Science Centre under Contract No. 2019/35/O/ST2/02907; The Swedish Research Council; and U.S. Department of Energy under Contract No. DE-FG02-05ER41374.

[1] S. K. Choi *et al.* (Belle Collaboration), Phys. Rev. Lett. **91**, 262001 (2003).
[2] B. Aubert *et al.* (*BABAR* Collaboration), Phys. Rev. Lett. **95**, 142001 (2005).
[3] M. Ablikim *et al.* (BESIII Collaboration), Phys. Rev. Lett. **110**, 252001 (2013).
[4] N. Brambilla *et al.*, Eur. Phys. J. C **71**, 1534 (2011).
[5] H. X. Chen, W. Chen, X. Liu, and S. L. Zhu, Phys. Rep. **639**, 1 (2016).
[6] Y. R. Liu, H. X. Chen, W. Chen, X. Liu, and S. L. Zhu, Prog. Part. Nucl. Phys. **107**, 237 (2019).
[7] N. Brambilla, S. Eidelman, C. Hanhart, A. Nefediev, C. P. Shen, C. E. Thomas, A. Vairo, and C. Z. Yuan, Phys. Rep. **873**, 1 (2020).
[8] R. L. Workman *et al.* (Particle Data Group), Prog. Theor. Exp. Phys. **2022**, 083C01 (2022).
[9] B. Aubert *et al.* (*BABAR* Collaboration), Phys. Rev. Lett. **98**, 212001 (2007).
[10] M. Ablikim *et al.* (BESIII Collaboration), Chin. Phys. C **46**, 111002 (2022).
[11] X. L. Wang *et al.* (Belle Collaboration), Phys. Rev. Lett. **99**, 142002 (2007).
[12] M. Ablikim *et al.* (BESIII Collaboration), Phys. Rev. Lett. **131**, 151903 (2023).
[13] M. Ablikim *et al.* (BESIII Collaboration), Phys. Rev. D **93**, 011102 (2016).
[14] M. Ablikim *et al.* (BESIII Collaboration), Nucl. Instrum. Methods Phys. Res., Sect. A **614**, 345 (2010).
[15] C. H. Yu *et al.*, in *Proceedings of IPAC2016, Busan, Korea* (JACoW, 2016), 10.18429/JACoW-IPAC2016-TUYA01.
[16] X. Li *et al.*, Radiat. Detect. Tech. Methods **1**, 13 (2017); Y. X. Guo *et al.*, Radiat. Detect. Tech. Methods **1**, 15 (2017).
[17] M. Ablikim *et al.* (BESIII Collaboration), Chin. Phys. C **39**, 093001 (2015).
[18] M. Ablikim *et al.* (BESIII Collaboration), Chin. Phys. C **45**, 103001 (2021).
[19] M. Ablikim *et al.* (BESIII Collaboration), Chin. Phys. C **46**, 113003 (2022).
[20] See Supplemental Material at http://link.aps.org/supplemental/10.1103/PhysRevLett.132.161901 for energies and luminosities of datasets and the obtained Born cross sections at different energy points.
[21] S. Actis *et al.* (Working Group on Radiative Corrections and Monte Carlo Generators for Low Energies Collaborations), Eur. Phys. J. C **66**, 585 (2010).
[22] S. Jadach, B. F. L. Ward, and Z. Was, Phys. Rev. D **63**, 113009 (2001); Comput. Phys. Commun. **130**, 260 (2000).
[23] E. A. Kuraev and V. S. Fadin, Sov. J. Nucl. Phys. **41**, 466 (1985), https://api.semanticscholar.org/CorpusID:124372625.
[24] W. Sun, T. Liu, M. Jing, L. Wang, B. Zhong, and W. Song, Front. Phys. **16**, 64501 (2021).
[25] M. Ablikim *et al.* (BESIII Collaboration), Phys. Rev. D **104**, 012001 (2021).
[26] M. Ablikim *et al.* (BESIII Collaboration), Phys. Rev. D **103**, L091102 (2021).
[27] M. Ablikim *et al.* (BESIII Collaboration), Phys. Rev. D **87**, 012002 (2013).
[28] M. Ablikim *et al.* (BESIII Collaboration), Phys. Rev. D **101**, 012008 (2020).
[29] M. Ablikim *et al.* (BESIII Collaboration), Phys. Rev. D **103**, 112004 (2021).
[30] M. Ablikim *et al.* (BESIII Collaboration), Chin. Phys. C **40**, 063001 (2016).
[31] M. Ablikim *et al.* (BESIII Collaboration), Phys. Rev. Lett. **130**, 121901 (2023).

M. Ablikim,[1] M. N. Achasov,[5,b] P. Adlarson,[75] X. C. Ai,[81] R. Aliberti,[36] A. Amoroso,[74a,74c] M. R. An,[40] Q. An,[71,58] Y. Bai,[57] O. Bakina,[37] I. Balossino,[30a] Y. Ban,[47,g] H.-R. Bao,[63] V. Batozskaya,[1,45] K. Begzsuren,[33] N. Berger,[36] M. Berlowski,[45] M. Bertani,[29a] D. Bettoni,[30a] F. Bianchi,[74a,74c] E. Bianco,[74a,74c] A. Bortone,[74a,74c] I. Boyko,[37] R. A. Briere,[6] A. Brueggemann,[68] H. Cai,[76] X. Cai,[1,58] A. Calcaterra,[29a] G. F. Cao,[1,63] N. Cao,[1,63] S. A. Cetin,[62a] J. F. Chang,[1,58] T. T. Chang,[77] W. L. Chang,[1,63] G. R. Che,[44] G. Chelkov,[37,a] C. Chen,[44] Chao Chen,[55] G. Chen,[1] H. S. Chen,[1,63] M. L. Chen,[1,58,63] S. J. Chen,[43] S. L. Chen,[46] S. M. Chen,[61] T. Chen,[1,63] X. R. Chen,[32,63] X. T. Chen,[1,63] Y. B. Chen,[1,58] Y. Q. Chen,[35] Z. J. Chen,[26,h] W. S. Cheng,[74c] S. K. Choi,[11] X. Chu,[44] G. Cibinetto,[30a] S. C. Coen,[4] F. Cossio,[74c] J. J. Cui,[50]

H. L. Dai,[1,58] J. P. Dai,[79] A. Dbeyssi,[19] R. E. de Boer,[4] D. Dedovich,[37] Z. Y. Deng,[1] A. Denig,[36] I. Denysenko,[37] M. Destefanis,[74a,74c] F. De Mori,[74a,74c] B. Ding,[66,1] X. X. Ding,[47,g] Y. Ding,[41] Y. Ding,[35] J. Dong,[1,58] L. Y. Dong,[1,63] M. Y. Dong,[1,58,63] X. Dong,[76] M. C. Du,[1] S. X. Du,[81] Z. H. Duan,[43] P. Egorov,[37,a] Y. H. Fan,[46] J. Fang,[1,58] S. S. Fang,[1,63] W. X. Fang,[1] Y. Fang,[1] R. Farinelli,[30a] L. Fava,[74b,74c] F. Feldbauer,[4] G. Felici,[29a] C. Q. Feng,[71,58] J. H. Feng,[59] K. Fischer,[69] M. Fritsch,[4] C. D. Fu,[1] J. L. Fu,[63] Y. W. Fu,[1] H. Gao,[63] Y. N. Gao,[47,g] Yang Gao,[71,58] S. Garbolino,[74c] I. Garzia,[30a,30b] P. T. Ge,[76] Z. W. Ge,[43] C. Geng,[59] E. M. Gersabeck,[67] A. Gilman,[69] K. Goetzen,[14] L. Gong,[41] W. X. Gong,[1,58] W. Gradl,[36] S. Gramigna,[30a,30b] M. Greco,[74a,74c] M. H. Gu,[1,58] Y. T. Gu,[16] C. Y. Guan,[1,63] Z. L. Guan,[23] A. Q. Guo,[32,63] L. B. Guo,[42] M. J. Guo,[50] R. P. Guo,[49] Y. P. Guo,[13,f] A. Guskov,[37,a] T. T. Han,[50] W. Y. Han,[40] X. Q. Hao,[20] F. A. Harris,[65] K. K. He,[55] K. L. He,[1,63] F. H. H. Heinsius,[4] C. H. Heinz,[36] Y. K. Heng,[1,58,63] C. Herold,[60] T. Holtmann,[4] P. C. Hong,[13,f] G. Y. Hou,[1,63] X. T. Hou,[1,63] Y. R. Hou,[63] Z. L. Hou,[1] H. M. Hu,[1,63] J. F. Hu,[56,i] T. Hu,[1,58,63] Y. Hu,[1] G. S. Huang,[71,58] K. X. Huang,[59] L. Q. Huang,[32,63] X. T. Huang,[50] Y. P. Huang,[1] T. Hussain,[73] N. Hüsken,[28,36] N. in der Wiesche,[68] M. Irshad,[71,58] J. Jackson,[28] S. Jaeger,[4] S. Janchiv,[33] J. H. Jeong,[11] Q. Ji,[1] Q. P. Ji,[20] X. B. Ji,[1,63] X. L. Ji,[1,58] Y. Y. Ji,[50] X. Q. Jia,[50] Z. K. Jia,[71,58] H. J. Jiang,[76] P. C. Jiang,[47,g] S. S. Jiang,[40] T. J. Jiang,[17] X. S. Jiang,[1,58,63] Y. Jiang,[63] J. B. Jiao,[50] Z. Jiao,[24] S. Jin,[43] Y. Jin,[66] M. Q. Jing,[1,63] X. M. Jing,[63] T. Johansson,[75] X. K.,[1] S. Kabana,[34] N. Kalantar-Nayestanaki,[64] X. L. Kang,[10] X. S. Kang,[41] M. Kavatsyuk,[64] B. C. Ke,[81] A. Khoukaz,[68] R. Kiuchi,[1] R. Kliemt,[14] O. B. Kolcu,[62a] B. Kopf,[4] M. Kuessner,[4] A. Kupsc,[45,75] W. Kühn,[38] J. J. Lane,[67] P. Larin,[19] A. Lavania,[27] L. Lavezzi,[74a,74c] T. T. Lei,[71,58] Z. H. Lei,[71,58] H. Leithoff,[36] M. Lellmann,[36] T. Lenz,[36] C. Li,[48] C. Li,[44] C. H. Li,[40] Cheng Li,[71,58] D. M. Li,[81] F. Li,[1,58] G. Li,[1] H. Li,[71,58] H. B. Li,[1,63] H. J. Li,[20] H. N. Li,[56,i] Hui Li,[44] J. R. Li,[61] J. S. Li,[59] J. W. Li,[50] K. L. Li,[20] Ke Li,[1] L. J. Li,[1,63] L. K. Li,[1] Lei Li,[3] M. H. Li,[44] P. R. Li,[39,j,k] Q. X. Li,[50] S. X. Li,[13] T. Li,[50] W. D. Li,[1,63] W. G. Li,[1] X. H. Li,[71,58] X. L. Li,[50] Xiaoyu Li,[1,63] Y. G. Li,[47,g] Z. J. Li,[59] Z. X. Li,[16] C. Liang,[43] H. Liang,[35] H. Liang,[71,58] H. Liang,[1,63] Y. F. Liang,[54] Y. T. Liang,[32,63] G. R. Liao,[15] L. Z. Liao,[50] Y. P. Liao,[1,63] J. Libby,[27] A. Limphirat,[60] D. X. Lin,[32,63] T. Lin,[1] B. J. Liu,[1] B. X. Liu,[76] C. Liu,[35] C. X. Liu,[1] F. H. Liu,[53] Fang Liu,[1] Feng Liu,[7] G. M. Liu,[56,i] H. Liu,[39,j,k] H. B. Liu,[16] H. M. Liu,[1,63] Huanhuan Liu,[1] Huihui Liu,[22] J. B. Liu,[71,58] J. L. Liu,[72] J. Y. Liu,[1,63] K. Liu,[1] K. Y. Liu,[41] Ke Liu,[23] L. Liu,[71,58] L. C. Liu,[44] Lu Liu,[44] M. H. Liu,[13,f] P. L. Liu,[1] Q. Liu,[63] S. B. Liu,[71,58] T. Liu,[13,f] W. K. Liu,[44] W. M. Liu,[71,58] X. Liu,[39,j,k] Y. Liu,[39,j,k] Y. Liu,[81] Y. B. Liu,[44] Z. A. Liu,[1,58,63] Z. Q. Liu,[50] X. C. Lou,[1,58,63] F. X. Lu,[59] H. J. Lu,[24] J. G. Lu,[1,58] X. L. Lu,[1] Y. Lu,[8] Y. P. Lu,[1,58] Z. H. Lu,[1,63] C. L. Luo,[42] M. X. Luo,[80] T. Luo,[13,f] X. L. Luo,[1,58] X. R. Lyu,[63] Y. F. Lyu,[44] F. C. Ma,[41] H. Ma,[79] H. L. Ma,[1] J. L. Ma,[1,63] L. L. Ma,[50] M. M. Ma,[1,63] Q. M. Ma,[1] R. Q. Ma,[1,63] R. T. Ma,[63] X. Y. Ma,[1,58] Y. Ma,[47,g] Y. M. Ma,[32] F. E. Maas,[19] M. Maggiora,[74a,74c] S. Malde,[69] Q. A. Malik,[73] A. Mangoni,[29b] Y. J. Mao,[47,g] Z. P. Mao,[1] S. Marcello,[74a,74c] Z. X. Meng,[66] J. G. Messchendorp,[14,64] G. Mezzadri,[30a] H. Miao,[1,63] T. J. Min,[43] R. E. Mitchell,[28] X. H. Mo,[1,58,63] N. Yu. Muchnoi,[5,b] J. Muskalla,[36] Y. Nefedov,[37] F. Nerling,[19,d] I. B. Nikolaev,[5,b] Z. Ning,[1,58] S. Nisar,[12,l] Q. L. Niu,[39,j,k] W. D. Niu,[55] Y. Niu,[50] S. L. Olsen,[63] Q. Ouyang,[1,58,63] S. Pacetti,[29b,29c] X. Pan,[55] Y. Pan,[57] A. Pathak,[35] P. Patteri,[29a] Y. P. Pei,[71,58] M. Pelizaeus,[4] H. P. Peng,[71,58] Y. Y. Peng,[39,j,k] K. Peters,[14,d] J. L. Ping,[42] R. G. Ping,[1,63] S. Plura,[36] V. Prasad,[34] F. Z. Qi,[1] H. Qi,[71,58] H. R. Qi,[61] M. Qi,[43] T. Y. Qi,[13,f] S. Qian,[1,58] W. B. Qian,[63] C. F. Qiao,[63] J. J. Qin,[72] L. Q. Qin,[15] X. P. Qin,[13,f] X. S. Qin,[50] Z. H. Qin,[1,58] J. F. Qiu,[1] S. Q. Qu,[61] C. F. Redmer,[36] K. J. Ren,[40] A. Rivetti,[74c] M. Rolo,[74c] G. Rong,[1,63] Ch. Rosner,[19] S. N. Ruan,[44] N. Salone,[45] A. Sarantsev,[37,c] Y. Schelhaas,[36] K. Schoenning,[75] M. Scodeggio,[30a,30b] K. Y. Shan,[13,f] W. Shan,[25] X. Y. Shan,[71,58] J. F. Shangguan,[55] L. G. Shao,[1,63] M. Shao,[71,58] C. P. Shen,[13,f] H. F. Shen,[1,63] W. H. Shen,[63] X. Y. Shen,[1,63] B. A. Shi,[63] H. C. Shi,[71,58] J. L. Shi,[13] J. Y. Shi,[1] Q. Q. Shi,[55] R. S. Shi,[1,63] X. Shi,[1,58] J. J. Song,[20] T. Z. Song,[59] W. M. Song,[35,1] Y. J. Song,[13] Y. X. Song,[47,g] S. Sosio,[74a,74c] S. Spataro,[74a,74c] F. Stieler,[36] Y. J. Su,[63] G. B. Sun,[76] G. X. Sun,[1] H. Sun,[63] H. K. Sun,[1] J. F. Sun,[20] K. Sun,[61] L. Sun,[76] S. S. Sun,[1,63] T. Sun,[1,63] W. Y. Sun,[35] Y. Sun,[10] Y. J. Sun,[71,58] Y. Z. Sun,[1] Z. T. Sun,[50] Y. X. Tan,[71,58] C. J. Tang,[54] G. Y. Tang,[1] J. Tang,[59] Y. A. Tang,[76] L. Y. Tao,[72] Q. T. Tao,[26,h] M. Tat,[69] J. X. Teng,[71,58] V. Thoren,[75] W. H. Tian,[59] W. H. Tian,[52] Y. Tian,[32,63] Z. F. Tian,[76] I. Uman,[62b] S. J. Wang,[50] B. Wang,[1] B. L. Wang,[63] Bo Wang,[71,58] C. W. Wang,[43] D. Y. Wang,[47,g] F. Wang,[72] H. J. Wang,[39,j,k] H. P. Wang,[1,63] J. P. Wang,[50] K. Wang,[1,58] L. L. Wang,[1] M. Wang,[50] Meng Wang,[1,63] S. Wang,[13,f] S. Wang,[39,j,k] T. Wang,[13,f] T. J. Wang,[44] W. Wang,[72] W. Wang,[59] W. P. Wang,[71,58] X. Wang,[47,g] X. F. Wang,[39,j,k] X. J. Wang,[40] X. L. Wang,[13,f] Y. Wang,[61] Y. D. Wang,[46] Y. F. Wang,[1,58,63] Y. H. Wang,[48] Y. N. Wang,[46] Y. Q. Wang,[1] Yaqian Wang,[18,1] Yi Wang,[61] Z. Wang,[1,58] Z. L. Wang,[72] Z. Y. Wang,[1,63] Ziyi Wang,[63] D. Wei,[70] D. H. Wei,[15] F. Weidner,[68] S. P. Wen,[1] C. W. Wenzel,[4] U. Wiedner,[4] G. Wilkinson,[69] M. Wolke,[75] L. Wollenberg,[4] C. Wu,[40] J. F. Wu,[1,63] L. H. Wu,[1] L. J. Wu,[1,63] X. Wu,[13,f] X. H. Wu,[35] Y. Wu,[71] Y. H. Wu,[55] Y. J. Wu,[32] Z. Wu,[1,58] L. Xia,[71,58] X. M. Xian,[40] T. Xiang,[47,g] D. Xiao,[39,j,k] G. Y. Xiao,[43] S. Y. Xiao,[1] Y. L. Xiao,[13,f] Z. J. Xiao,[42] C. Xie,[43] X. H. Xie,[47,g] Y. Xie,[50] Y. G. Xie,[1,58] Y. H. Xie,[7] Z. P. Xie,[71,58] T. Y. Xing,[1,63] C. F. Xu,[1,63] C. J. Xu,[59] G. F. Xu,[1] H. Y. Xu,[66] Q. J. Xu,[17] Q. N. Xu,[31]

W. Xu,[1,63] W. L. Xu,[66] X. P. Xu,[55] Y. C. Xu,[78] Z. P. Xu,[43] Z. S. Xu,[63] F. Yan,[13,f] L. Yan,[13,f] W. B. Yan,[71,58] W. C. Yan,[81]
X. Q. Yan,[1] H. J. Yang,[51,e] H. L. Yang,[35] H. X. Yang,[1] Tao Yang,[1] Y. Yang,[13,f] Y. F. Yang,[44] Y. X. Yang,[1,63] Yifan Yang,[1,63]
Z. W. Yang,[39,j,k] Z. P. Yao,[50] M. Ye,[1,58] M. H. Ye,[9] J. H. Yin,[1] Z. Y. You,[59] B. X. Yu,[1,58,63] C. X. Yu,[44] G. Yu,[1,63] J. S. Yu,[26,h]
T. Yu,[72] X. D. Yu,[47,g] C. Z. Yuan,[1,63] L. Yuan,[2] S. C. Yuan,[1] X. Q. Yuan,[1] Y. Yuan,[1,63] Z. Y. Yuan,[59] C. X. Yue,[40]
A. A. Zafar,[73] F. R. Zeng,[50] X. Zeng,[13,f] Y. Zeng,[26,h] Y. J. Zeng,[1,63] X. Y. Zhai,[35] Y. C. Zhai,[50] Y. H. Zhan,[59] A. Q. Zhang,[1,63]
B. L. Zhang,[1,63] B. X. Zhang,[1] D. H. Zhang,[44] G. Y. Zhang,[20] H. Zhang,[71] H. C. Zhang,[1,58,63] H. H. Zhang,[35] H. H. Zhang,[59]
H. Q. Zhang,[1,58,63] H. Y. Zhang,[1,58] J. Zhang,[81] J. J. Zhang,[52] J. L. Zhang,[21] J. Q. Zhang,[42] J. W. Zhang,[1,58,63] J. X. Zhang,[39,j,k]
J. Y. Zhang,[1] J. Z. Zhang,[1,63] Jianyu Zhang,[63] Jiawei Zhang,[1,63] L. M. Zhang,[61] L. Q. Zhang,[59] Lei Zhang,[43] P. Zhang,[1,63]
Q. Y. Zhang,[40,81] Shuihan Zhang,[1,63] Shulei Zhang,[26,h] X. D. Zhang,[46] X. M. Zhang,[1] X. Y. Zhang,[50] Xuyan Zhang,[55]
Y. Zhang,[69] Y. Zhang,[72] Y. T. Zhang,[81] Y. H. Zhang,[1,58] Yan Zhang,[71,58] Yao Zhang,[1] Z. H. Zhang,[1] Z. L. Zhang,[35]
Z. Y. Zhang,[76] Z. Y. Zhang,[44] G. Zhao,[1] J. Zhao,[40] J. Y. Zhao,[1,63] J. Z. Zhao,[1,58] Lei Zhao,[71,58] Ling Zhao,[1] M. G. Zhao,[44]
R. P. Zhao,[63] S. J. Zhao,[81] Y. B. Zhao,[1,58] Y. X. Zhao,[32,63] Z. G. Zhao,[71,58] A. Zhemchugov,[37,a] B. Zheng,[72] J. P. Zheng,[1,58]
W. J. Zheng,[1,63] Y. H. Zheng,[63] B. Zhong,[42] X. Zhong,[59] H. Zhou,[50] L. P. Zhou,[1,63] X. Zhou,[76] X. K. Zhou,[7] X. R. Zhou,[71,58]
X. Y. Zhou,[40] Y. Z. Zhou,[13,f] J. Zhu,[44] K. Zhu,[1] K. J. Zhu,[1,58,63] L. Zhu,[35] L. X. Zhu,[63] S. H. Zhu,[70] S. Q. Zhu,[43] T. J. Zhu,[13,f]
W. J. Zhu,[13,f] Y. C. Zhu,[71,58] Z. A. Zhu,[1,63] J. H. Zou,[1] and J. Zu[71,58]

(BESIII Collaboration)

[1]*Institute of High Energy Physics, Beijing 100049, People's Republic of China*
[2]*Beihang University, Beijing 100191, People's Republic of China*
[3]*Beijing Institute of Petrochemical Technology, Beijing 102617, People's Republic of China*
[4]*Bochum Ruhr-University, D-44780 Bochum, Germany*
[5]*Budker Institute of Nuclear Physics SB RAS (BINP), Novosibirsk 630090, Russia*
[6]*Carnegie Mellon University, Pittsburgh, Pennsylvania 15213, USA*
[7]*Central China Normal University, Wuhan 430079, People's Republic of China*
[8]*Central South University, Changsha 410083, People's Republic of China*
[9]*China Center of Advanced Science and Technology, Beijing 100190, People's Republic of China*
[10]*China University of Geosciences, Wuhan 430074, People's Republic of China*
[11]*Chung-Ang University, Seoul, 06974, Republic of Korea*
[12]*COMSATS University Islamabad, Lahore Campus, Defence Road, Off Raiwind Road, 54000 Lahore, Pakistan*
[13]*Fudan University, Shanghai 200433, People's Republic of China*
[14]*GSI Helmholtzcentre for Heavy Ion Research GmbH, D-64291 Darmstadt, Germany*
[15]*Guangxi Normal University, Guilin 541004, People's Republic of China*
[16]*Guangxi University, Nanning 530004, People's Republic of China*
[17]*Hangzhou Normal University, Hangzhou 310036, People's Republic of China*
[18]*Hebei University, Baoding 071002, People's Republic of China*
[19]*Helmholtz Institute Mainz, Staudinger Weg 18, D-55099 Mainz, Germany*
[20]*Henan Normal University, Xinxiang 453007, People's Republic of China*
[21]*Henan University, Kaifeng 475004, People's Republic of China*
[22]*Henan University of Science and Technology, Luoyang 471003, People's Republic of China*
[23]*Henan University of Technology, Zhengzhou 450001, People's Republic of China*
[24]*Huangshan College, Huangshan 245000, People's Republic of China*
[25]*Hunan Normal University, Changsha 410081, People's Republic of China*
[26]*Hunan University, Changsha 410082, People's Republic of China*
[27]*Indian Institute of Technology Madras, Chennai 600036, India*
[28]*Indiana University, Bloomington, Indiana 47405, USA*
[29a]*INFN Laboratori Nazionali di Frascati, INFN Laboratori Nazionali di Frascati, I-00044, Frascati, Italy*
[29b]*INFN Sezione di Perugia, I-06100, Perugia, Italy*
[29c]*University of Perugia, I-06100, Perugia, Italy*
[30a]*INFN Sezione di Ferrara, INFN Sezione di Ferrara, I-44122, Ferrara, Italy*
[30b]*University of Ferrara, I-44122, Ferrara, Italy*
[31]*Inner Mongolia University, Hohhot 010021, People's Republic of China*
[32]*Institute of Modern Physics, Lanzhou 730000, People's Republic of China*
[33]*Institute of Physics and Technology, Peace Avenue 54B, Ulaanbaatar 13330, Mongolia*
[34]*Instituto de Alta Investigación, Universidad de Tarapacá, Casilla 7D, Arica 1000000, Chile*

[35]*Jilin University, Changchun 130012, People's Republic of China*
[36]*Johannes Gutenberg University of Mainz, Johann-Joachim-Becher-Weg 45, D-55099 Mainz, Germany*
[37]*Joint Institute for Nuclear Research, 141980 Dubna, Moscow region, Russia*
[38]*Justus-Liebig-Universitaet Giessen, II. Physikalisches Institut, Heinrich-Buff-Ring 16, D-35392 Giessen, Germany*
[39]*Lanzhou University, Lanzhou 730000, People's Republic of China*
[40]*Liaoning Normal University, Dalian 116029, People's Republic of China*
[41]*Liaoning University, Shenyang 110036, People's Republic of China*
[42]*Nanjing Normal University, Nanjing 210023, People's Republic of China*
[43]*Nanjing University, Nanjing 210093, People's Republic of China*
[44]*Nankai University, Tianjin 300071, People's Republic of China*
[45]*National Centre for Nuclear Research, Warsaw 02-093, Poland*
[46]*North China Electric Power University, Beijing 102206, People's Republic of China*
[47]*Peking University, Beijing 100871, People's Republic of China*
[48]*Qufu Normal University, Qufu 273165, People's Republic of China*
[49]*Shandong Normal University, Jinan 250014, People's Republic of China*
[50]*Shandong University, Jinan 250100, People's Republic of China*
[51]*Shanghai Jiao Tong University, Shanghai 200240, People's Republic of China*
[52]*Shanxi Normal University, Linfen 041004, People's Republic of China*
[53]*Shanxi University, Taiyuan 030006, People's Republic of China*
[54]*Sichuan University, Chengdu 610064, People's Republic of China*
[55]*Soochow University, Suzhou 215006, People's Republic of China*
[56]*South China Normal University, Guangzhou 510006, People's Republic of China*
[57]*Southeast University, Nanjing 211100, People's Republic of China*
[58]*State Key Laboratory of Particle Detection and Electronics, Beijing 100049, Hefei 230026, People's Republic of China*
[59]*Sun Yat-Sen University, Guangzhou 510275, People's Republic of China*
[60]*Suranaree University of Technology, University Avenue 111, Nakhon Ratchasima 30000, Thailand*
[61]*Tsinghua University, Beijing 100084, People's Republic of China*
[62a]*Turkish Accelerator Center Particle Factory Group, Istinye University, 34010, Istanbul, Turkey*
[62b]*Near East University, Nicosia, North Cyprus, 99138, Mersin 10, Turkey*
[63]*University of Chinese Academy of Sciences, Beijing 100049, People's Republic of China*
[64]*University of Groningen, NL-9747 AA Groningen, The Netherlands*
[65]*University of Hawaii, Honolulu, Hawaii 96822, USA*
[66]*University of Jinan, Jinan 250022, People's Republic of China*
[67]*University of Manchester, Oxford Road, Manchester, M13 9PL, United Kingdom*
[68]*University of Muenster, Wilhelm-Klemm-Strasse 9, 48149 Muenster, Germany*
[69]*University of Oxford, Keble Road, Oxford OX13RH, United Kingdom*
[70]*University of Science and Technology Liaoning, Anshan 114051, People's Republic of China*
[71]*University of Science and Technology of China, Hefei 230026, People's Republic of China*
[72]*University of South China, Hengyang 421001, People's Republic of China*
[73]*University of the Punjab, Lahore-54590, Pakistan*
[74a]*University of Turin and INFN, University of Turin, I-10125, Turin, Italy*
[74b]*University of Eastern Piedmont, I-15121, Alessandria, Italy*
[74c]*INFN, I-10125, Turin, Italy*
[75]*Uppsala University, Box 516, SE-75120 Uppsala, Sweden*
[76]*Wuhan University, Wuhan 430072, People's Republic of China*
[77]*Xinyang Normal University, Xinyang 464000, People's Republic of China*
[78]*Yantai University, Yantai 264005, People's Republic of China*
[79]*Yunnan University, Kunming 650500, People's Republic of China*
[80]*Zhejiang University, Hangzhou 310027, People's Republic of China*
[81]*Zhengzhou University, Zhengzhou 450001, People's Republic of China*

[a] Also at the Moscow Institute of Physics and Technology, Moscow 141700, Russia.

[b] Also at the Novosibirsk State University, Novosibirsk, 630090, Russia.

[c] Also at the NRC "Kurchatov Institute," PNPI, 188300, Gatchina, Russia.

[d] Also at Goethe University Frankfurt, 60323 Frankfurt am Main, Germany.

[e] Also at Key Laboratory for Particle Physics, Astrophysics and Cosmology, Ministry of Education; Shanghai Key Laboratory for Particle Physics and Cosmology; Institute of Nuclear and Particle Physics, Shanghai 200240, People's Republic of China.

[f] Also at Key Laboratory of Nuclear Physics and Ion-beam Application (MOE) and Institute of Modern Physics, Fudan University, Shanghai 200443, People's Republic of China.

[g] Also at State Key Laboratory of Nuclear Physics and Technology, Peking University, Beijing 100871, People's Republic of China.

[h] Also at School of Physics and Electronics, Hunan University, Changsha 410082, China.

[i] Also at Guangdong Provincial Key Laboratory of Nuclear Science, Institute of Quantum Matter, South China Normal University, Guangzhou 510006, China.

[j] Also at Frontiers Science Center for Rare Isotopes, Lanzhou University, Lanzhou 730000, People's Republic of China.

[k] Also at Lanzhou Center for Theoretical Physics, Lanzhou University, Lanzhou 730000, People's Republic of China.

[l] Also at the Department of Mathematical Sciences, IBA, Karachi 75270, Pakistan.